Supplement of Atmos. Chem. Phys., 26, 1795–1807, 2026
https://doi.org/10.5194/acp-26-1795-2026-supplement

Atmospheric Chemistry and Physics
Open Access

Supplement of

Driving factors for the activity coefficient of atmospheric ammonium nitrate: discrepancies among thermodynamic models and impact on nitrate pollutions

Ruilin Wan et al.

Correspondence to: Guangjie Zheng (zgj123@mail.tsinghua.edu.cn)

S1 Influence of γ_{AN}^2 on nitrate partitioning in ISORROPIA

For the NH_3-H_2SO_4-HNO_3-H_2O system, ISORROPIA operates under subcase "D3". When a small amount of Na^+ is introduced, forming Na^+-NH_3-H_2SO_4-HNO_3-H_2O system, the calculation procedure of ISORROPIA shifts from "D3" to "G5". In both subcases γ_{AN}^2 plays a critical role when solving HNO_3-NO_3^- gas-particle partitioning and is detailed in Zheng's previous study[1].

Briefly, for the subcase "D3", the major equilibriums considered is the gas-particle partitioning of ammonia and nitrates, which are:

$$C_1 = \frac{[NO_3^-(aq)][NH_4^+(aq)]}{[HNO_3(g)][NH_3(g)]} = \frac{K_{ag,HNO_3}}{K_{ag,NH_3}\gamma_{AN}^2} \quad \text{(Eq. S1)}$$

As shown in the equation, the only activity coefficients that matters in solving of NH_3-H_2SO_4-HNO_3-H_2O is γ_{AN}^2 in C_1.

For the subcase "G5", the major equilibriums considered are the gas-particle partitioning of NH_3, HNO_3 and HCl, which are:

$$C_2 = \frac{[NO_3^-(aq)][HCl(g)]}{[Cl^-(aq)][HNO_3(g)]} = \frac{K_{ag,HNO_3}}{K_{ag,HCl}} \frac{\gamma_{H-Cl}^2}{\gamma_{H-NO3}^2} \quad \text{(Eq. S2)}$$

$$[\mathrm{NH_4^+(aq)}]^2 - \mathrm{B}[\mathrm{NH_4^+(aq)}] + \mathrm{C} = 0 \quad \text{(Eq. S3)}$$

where

$$\mathrm{B} = [\mathrm{NH_3}]_\mathrm{t} + [\mathrm{Na^+}] - 2[\mathrm{H_2SO_4}]_\mathrm{t} + [\mathrm{Cl^-(aq)}] + [\mathrm{NO_3^-(aq)}] + \mathrm{C_3^{-1}}$$

$C = [NH_3]_t + [Na^+] - 2([H_2SO_4]_t)([Cl^-(aq)] + [NO_3^-(aq)]) - C_3^{-1}(2[H_2SO_4]_t - [Na^+])$.

The $[NH_4^+(aq)]$ is associated with $Cl^-(aq)$ and $NO_3^-(aq)$, whose solution includes $C_3 = \frac{\gamma^2_{H-NO_3(aq)}}{K_{ag,\ NH_3}\ \gamma^2_{AN}}$ as shown in Zheng's work([1]). Therefore, γ^2_{AN} also matters in solving gas-particle partitioning of Na^+-NH_3-H_2SO_4-HNO_3-H_2O system.

S2 Comparison of γ^2_{AN} of AIOMFAC with E-AIM and ISORROPIA as input

The γ^2_{AN} outputs of AIOMFAC with ISORROPIA and E-AIM as input respectively are compared in Fig. S1(a), which proved that there's no significant difference when the two models' outputs are as inputs. However, the presence of non-zero Na^+ in inputs in Na^+-NH_3-H_2SO_4-HNO_3-H_2O scenario triggers ISORROPIA to invoke the ISRP3F subroutine, which is automatically activated when either Na^+ or Cl is present in the input[2]. Consequently, ISORROPIA produces outputs that violate ion mass balance, with Cl^- appearing in the output despite being absent from the input. In contrast, this issue does not occur in E-AIM.

S3 Comparison of related variables

As depicted in Fig.S2a~c, for the estimation of ionic strength IS, f_{NVC}, and f_{NO3^-}, the results obtained from AIOMFAC show perfect consistency with those from E-AIM. Since the AIOMFAC model does not require RH data as input, it calculates the system RH at equilibrium thermodynamically. Therefore, comparing the RH consistency

between AIOMFAC and E-AIM can serve as an indirect assessment of the accuracy of the AIOMFAC model. As shown in Fig. S2d, for RH estimation, AIOMFAC and E-AIM show overall consistency. However, the discrepancy between the two expands as RH decreases, with better agreement at higher RH and larger discrepancies at lower RH. ISORROPIA results align well with E-AIM for the estimation of f_{NVC} and f_{NO3-}, as illustrated in Fig. S2f, g. For IS estimation, ISORROPIA demonstrates a certain degree of underestimation (see Fig. S2e). Ridge regression analysis reveals that the differences in IS between the two models are primarily due to discrepancies in the estimation of semi-volatile species such as NO_3^- and NH_4^+, and partially ionized substance pair, i.e., HSO_4^- and SO_4^{2-} (see Fig. S3-4).

Supplementary Figures

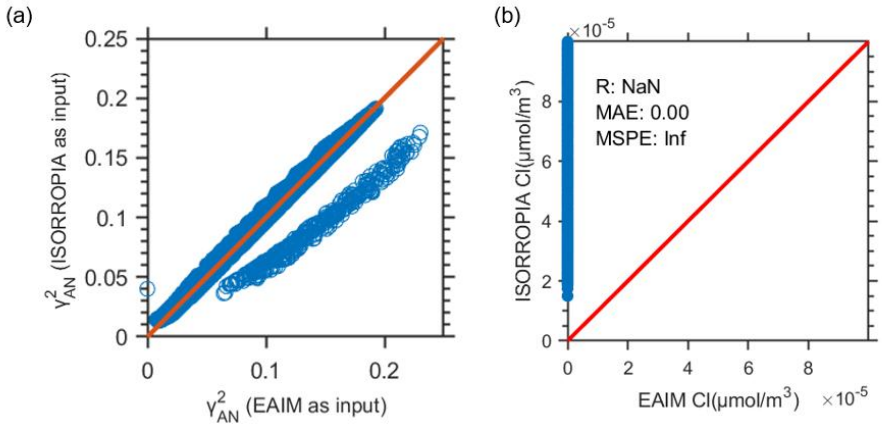

Figure S1. (a) γ^2_{AN} calculated by AIOMFAC with different inputs from E-AIM and ISORROPIA output in Scenario Met. The distinguishing differentiated branch corresponds to the IS differentiated branch shown in Fig. S2e. (b) Comparison of output Cl^- concentration(μmol/m^3) between ISORROPIA and E-AIM.

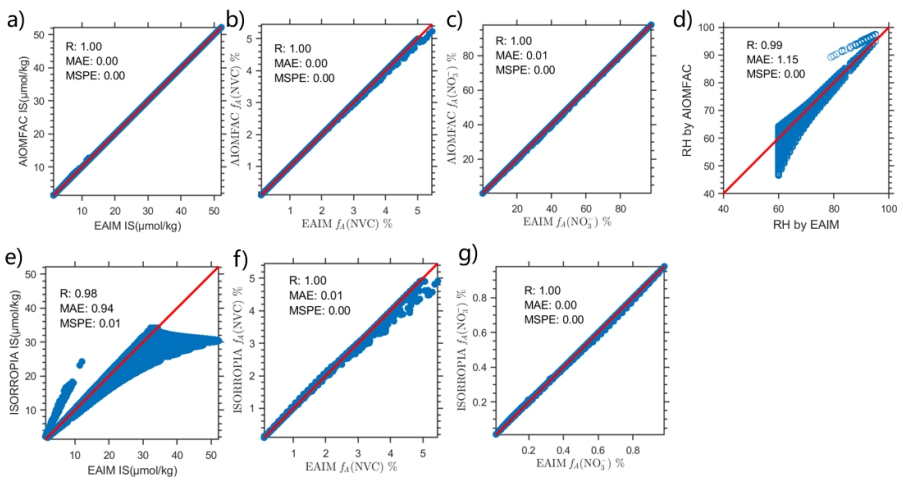

Figure S2. Scenario Met. related variables comparisons. Comparison (a ~ d) between AIOMFAC and E-AIM; (e ~ g) ISORROPIA and E-AIM in ionic strength IS (mol/kg), non-volatile cation fraction in anions f_{NVC}, nitrate fraction in anions f_{NO3-} and RH. R refers to Pearson correlation coefficient; MAE stands for mean absolute error; MSPE is short for mean squared percentage error.

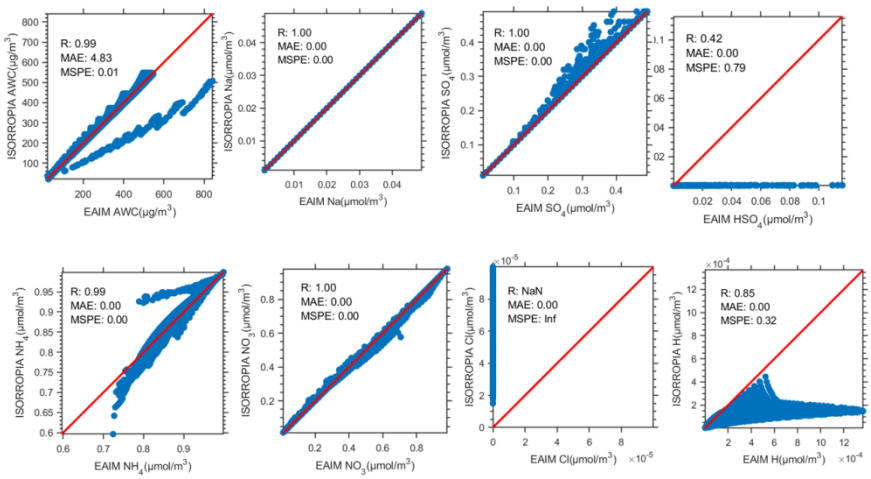

Figure S3. Comparison of species concentration estimated by ISORROPIA and E-AIM for Scenario Met.

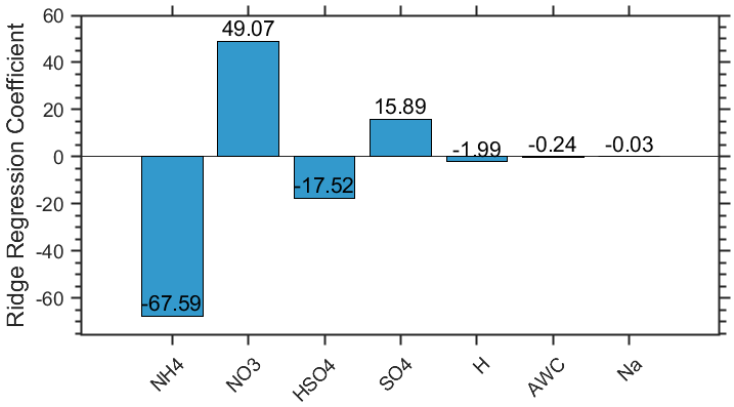

Figure S4. Ridge regression analysis of IS difference dominant influencing factors. Lamda choose 0.01 by using k-fold cross validation. Ridge regression coefficients representing the relative contributions of variable differences to IS difference. Positive coefficients (e.g., NO_3 and SO_4) indicate a positive association with IS difference, while negative coefficients (e.g., NH_4 and HSO_4) indicate a negative association. The magnitude reflects the strength of each variable's influence after standardization and regularization.

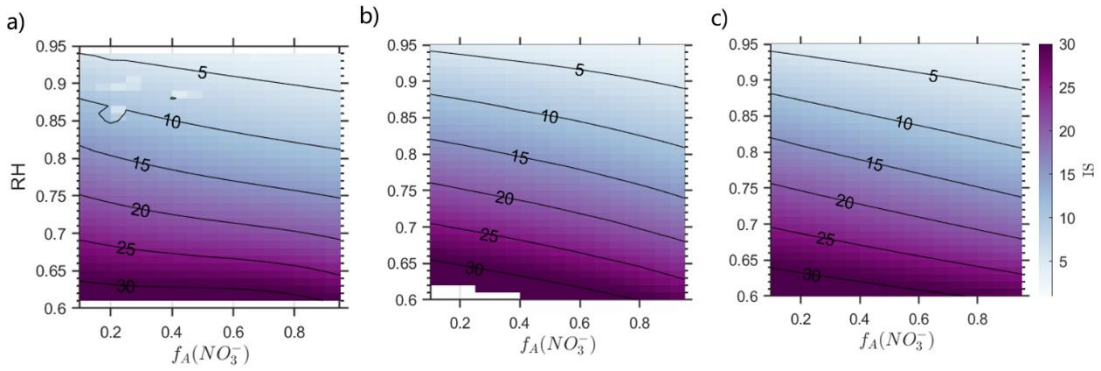

Figure S5. IS for Scenario Met. simulation under different f_{NO3-} and RH estimated by (a) E-AIM; (b) AIOMFAC; (c) ISORROPIA. T = 288K.

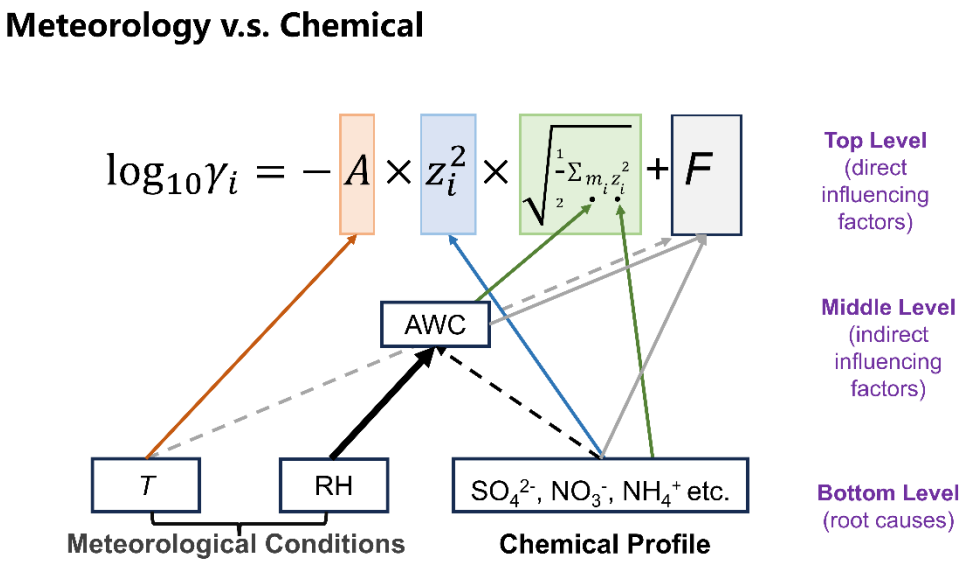

Figure S6. Hierarchical relationship among influencing factors of γ_i based on Debye-Hückel equation as established with the interpretive structural modeling approach. IS = $\frac{1}{2}\sum m_i z_i^2$(see main text Eq.5).

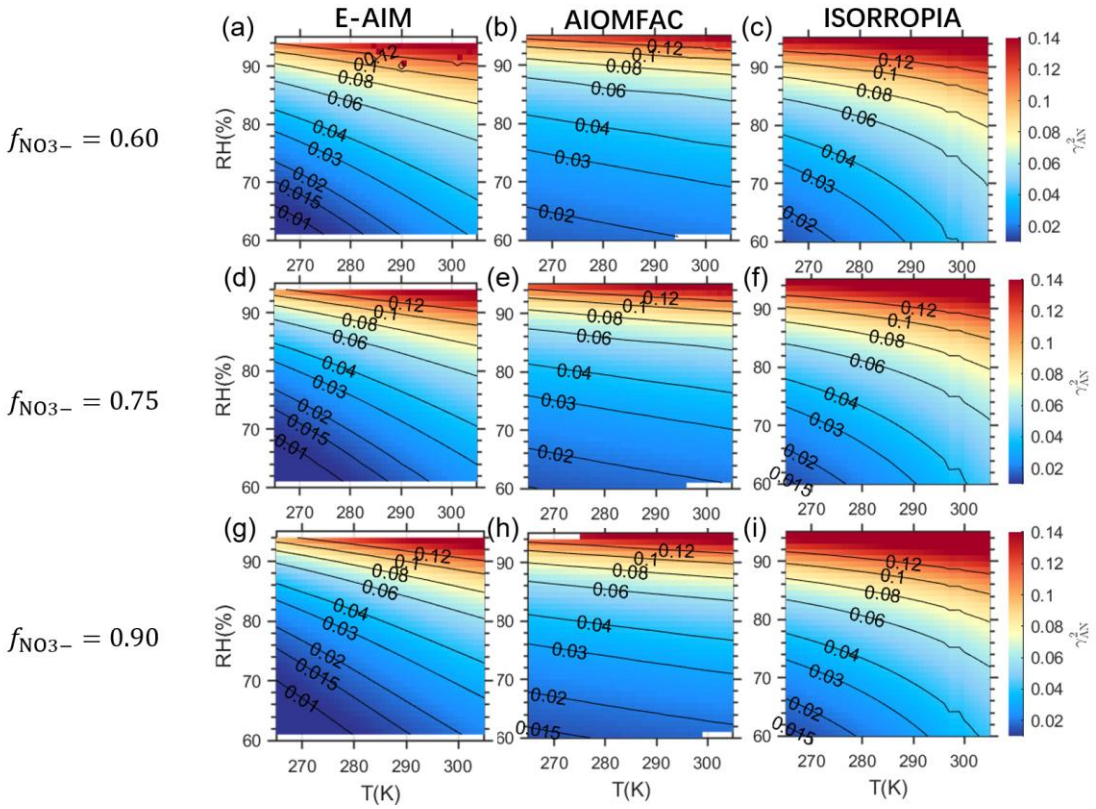

Figure S7. Comparison of the dependence of γ_{AN} on different influencing factors as estimated by (a, d, g) E-AIM; (b, e, h) AIOMFAC; (c, f, i) ISORROPIA. The γ^2_{AN} under different T and RH conditions, with (a-c) f_{NO3-} fixed at 0.60; (d-f) f_{NO3-} fixed at 0.75; (g-i) f_{NO3-} fixed at 0.90.

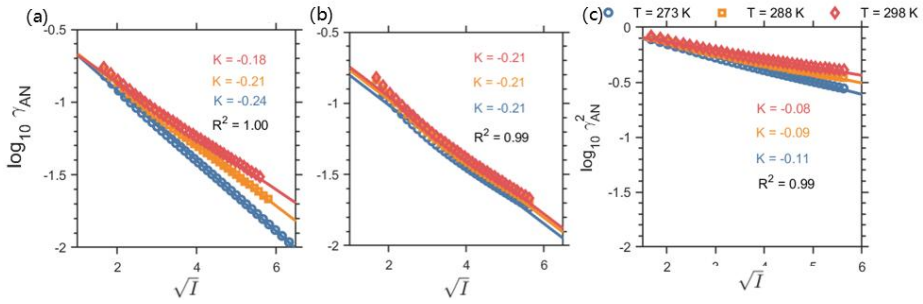

Figure S8. Dependence of γ_{AN} to IS in (a) E-AIM; (b) AIOMFAC; (c) ISORROPIA. By fixing the component concentration at f_{NO3-}=0.25, T=273K, 288K and 298K are divided into lower temperature, medium temperature and higher temperature.

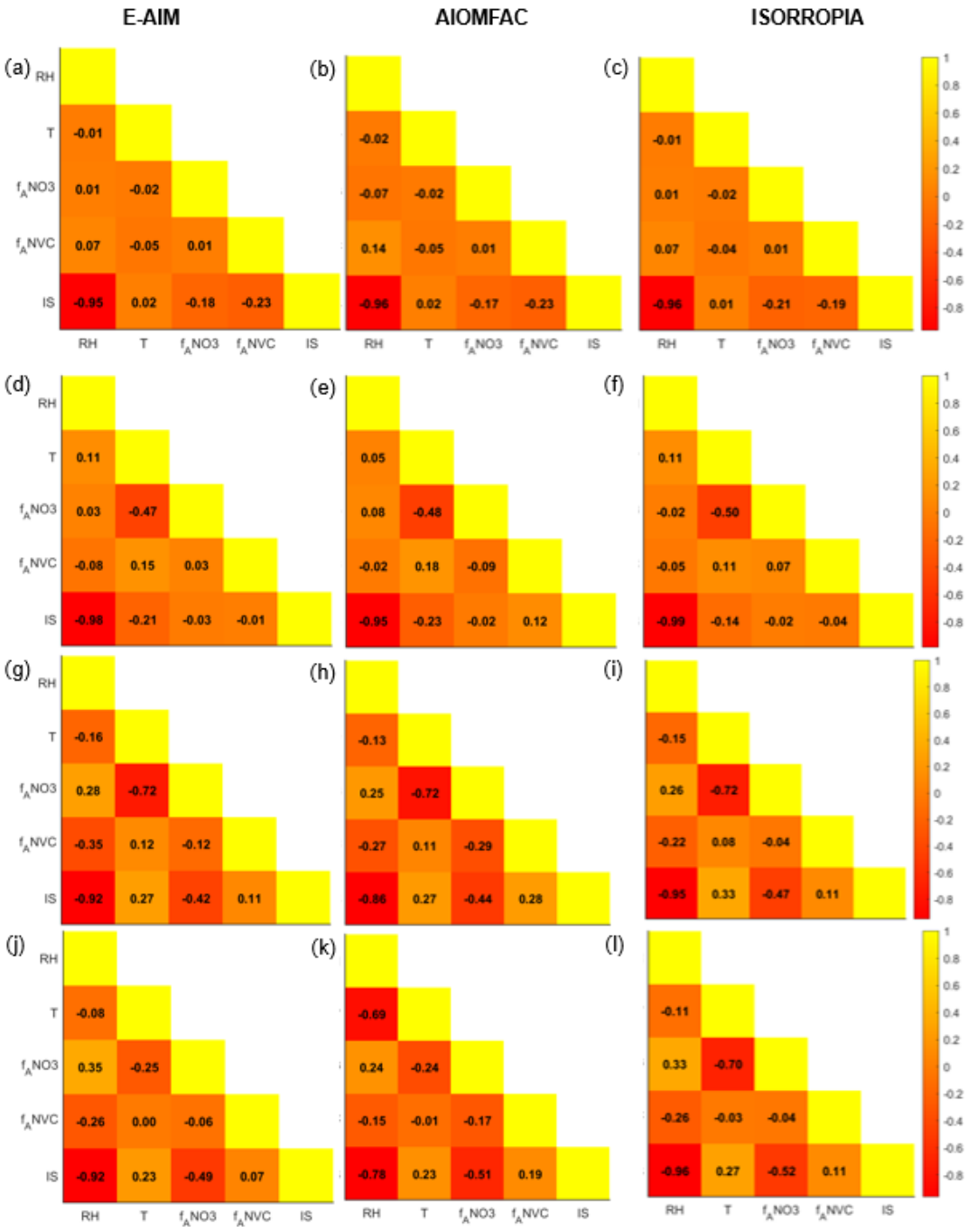

Figure S9. Relative influencing factors coefficients for (a ~ c) simulation data based on Scenario Full; (d ~ f) USA; (g ~ i) Canada; (j ~ l) China. The left, middle, and right columns correspond to the results from E-AIM, AIOMFAC, and ISORROPIA, respectively.

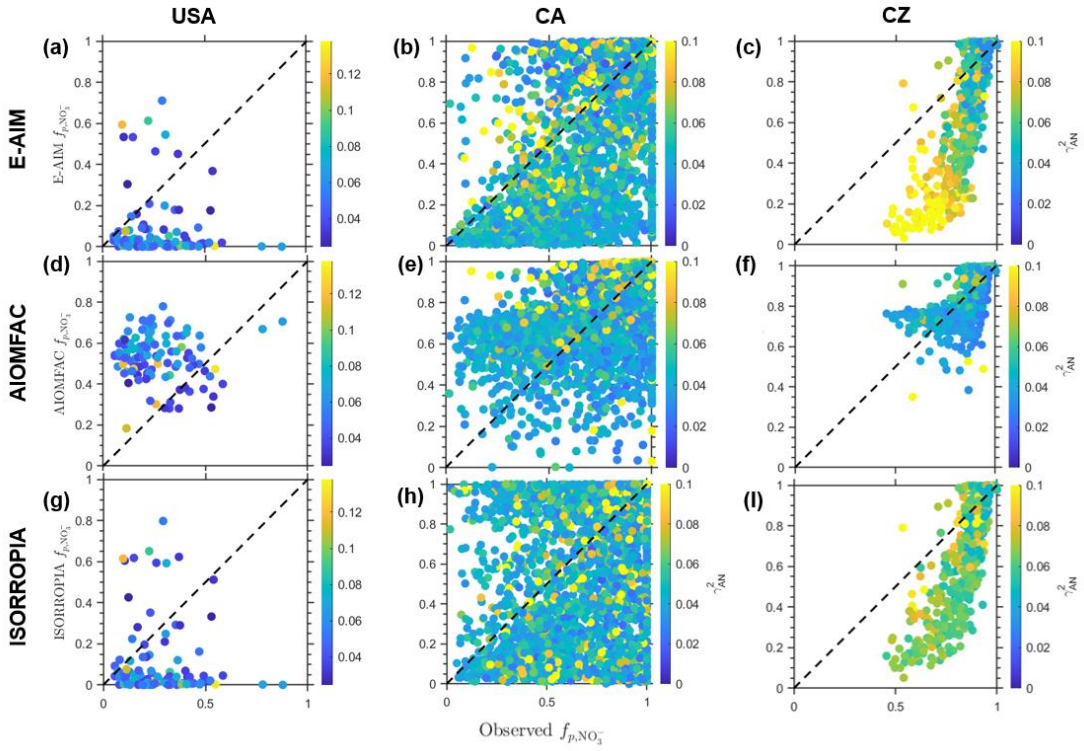

Figure S10. Comparisons of $f_{p}NO_3^-$ estimated by (a ~ c) E-AIM; (d ~ f) AIOMFAC; (g ~ i) ISORROPIA and observational data. The left, middle, and right panels correspond to the USA, Canada, and China, respectively. The scatter points are color-coded according to the model-predicted values of γ^2_{AN}.

Supplementary Tables

Table S1. Gibbs Energies of Formation

Substance and Physical state	$\mu 0, aq(g)_i$(J· mol^{-1})
HNO_3, g	-73.54
HNO_3, aq	-111.34
H^+, aq	0

The following apply:

$$K_{HNO_3} = \exp\left(\frac{\mu 0, g_{HNO_3} - \mu 0, aq_{NO_3^-} - \mu 0, aq_{H^+}}{RT}\right)$$

where $\mu 0, aq(g)_i$(J·mol^{-1}) is the Gibbs Energy of Formation of species *i*, R (J· K^{-1} ·mol^{-1}) is the universal gas constant, T(K) is temperature.

Table S2. Long-term observations of atmospheric composition and gas pollutants in three sites. All concentrations were averaged daily with the unit of $\mu g/m^3$.

Sites	**Centreville, US**	**Six sites in Canada**	**Changzhou, China**
Period	2010, 2012~2016	2007~2016	2018~2023
Gas pollutants	NH_3, HNO_3	NH_3, HNO_3	NH_3, HNO_3, HCl
Equivalent Na^+	0.13	0.14	0.08
SO_4^{2-}	1.80	1.67	1.28
$NH_{3,\ tot}$	0.54	2.50	2.31
$HNO_{3,\ tot}$	0.22	1.67	1.07
Cl^-	0.04	0.03	0.03
Average RH	0.77	0.76	0.79
Average temperature	293.20	283.13	282.01
Valid data number	504	3549	516
Ref.	[3,4]	[5]	[6]

Table S3. Comparison of γ_{AN}^2 sensitivity to cations and anions. Data are based on Scenario Chem.

RH	E-AIM		AIOMFAC		ISORROPIA	
	Mean sensitivity $f_{NO_3^-}$	Mean sensitivity f_{NVC}	Mean sensitivity $f_{NO_3^-}$	Mean sensitivity f_{NVC}	Mean sensitivity $f_{NO_3^-}$	Mean sensitivity f_{NVC}
60%	0.16	0.08	0.02	0.03	0.01	0.04
75%	0.12	0.06	0.01	0.03	0.01	0.04
90%	0.13	0.12	0.13	0.12	0.05	0.04

* "**mean sensitivity**" refers to the mean value of absolute $\frac{\partial \gamma_{AN}^2}{\partial f_{NO_3^-}}$ ($\frac{\partial \gamma_{AN}^2}{\partial f_{NVC}}$).

Additional Reference

1. Zheng, G., Su, H., Wang, S., Pozzer, A. & Cheng, Y. Impact of non-ideality on reconstructing spatial and temporal variations in aerosol acidity with multiphase buffer theory. *Atmos. Chem. Phys.* **22**, 47–63 (2022).
2. Fountoukis, C. & Nenes, A. ISORROPIA II: a computationally efficient thermodynamic equilibrium model for K+ – Ca2+ – Mg2+ – NH4+ – Na+ – SO42− – NO3− – Cl− – H2O aerosols. *Atmospheric Chemistry and Physics* **7**, 4639–4659 (2007).
3. Edgerton, E. S. *et al.* The Southeastern Aerosol Research and Characterization Study, Part 3: Continuous Measurements of Fine Particulate Matter Mass and Composition. *Journal of the Air & Waste Management Association* **56**, 1325–1341 (2006).
4. Hansen, D. A. *et al.* The Southeastern Aerosol Research and Characterization Study: Part 1—Overview. *Journal of the Air & Waste Management Association* **53**, 1460–1471 (2003).
5. Tao, Y. & Murphy, J. G. The sensitivity of $PM_{2.5}$ acidity to meteorological parameters and chemical composition changes: 10-year records from six Canadian monitoring sites. *Atmos. Chem. Phys.* **19**, 9309–9320 (2019).
6. Duan, X., Zheng, G., Chen, C., Zhang, Q. & He, K. Driving factors of aerosol acidity: a new hierarchical quantitative analysis framework and its application in Changzhou, China. Preprint at https://doi.org/10.5194/egusphere-2024-3584 (2024).